QCD corrections to J/ψ plus η_c production in e^+e^- annihilation at $\sqrt{s} = 10.6$ GeV

Bin Gong and Jian-Xiong Wang

Institute of High Energy Physics, Chinese Academy of Sciences, P.O. Box 918(4), Beijing, 100049, China

(Received 28 December 2007; revised manuscript received 19 February 2008; published 31 March 2008)

Next-to-leading-order QCD corrections to J/ψ plus η_c production in e^+e^- annihilation at $\sqrt{s} = 10.6$ GeV are calculated in this paper, and an analytic result is obtained. By choosing proper physical parameters, a K factor (ratio of next-to-leading order to LO) of about 2, which is in agreement with the result in Y.-J. Zhang, Y.-j. Gao, and K.-T. Chao, Phys. Rev. Lett. **96**, 092001 (2006), is obtained. The plot of the K factor vs the center-of-mass energy $\sqrt{s}$ shows that it is more difficult to obtain a convergent result from the perturbative QCD without resummation of $\ln(s/m_c^2)$ terms as the $\sqrt{s}$ becomes larger.

DOI: 10.1103/PhysRevD.77.054028 PACS numbers: 12.38.Bx, 13.66.Bc, 14.40.Gx

I. INTRODUCTION

Perturbative quantum chromodynamics calculations are essential in the effort to describe large momentum transfer processes. To apply it to heavy quarkonium physics, the nonrelativistic QCD (NRQCD) factorization approach [1] has been introduced. It allows a consistent theoretical prediction to be made and to be improved perturbatively in the QCD coupling constant α_s and the heavy-quark relative velocity v. However, the J/ψ polarization measurement at the Fermilab Tevatron in proton-antiproton collisions [2] and J/ψ production in B factories [3–5] have shown that the leading order (LO) theoretical predictions in NRQCD could not match the experimental results. The large discrepancy was found in the double charm production in e^+e^- annihilation at B factories. The exclusive production cross section of double charmonium in $e^+e^- \to J/\psi\eta_c$ at $\sqrt{s} = 10.6$ GeV measured by Belle [3,4] is $\sigma[J/\psi + \eta_c] \times B^{\eta_c}[\geq 2] = (25.6 \pm 2.8 \pm 3.4)$ fb, and by *BABAR* [5] it is $\sigma[J/\psi + \eta_c] \times B^{\eta_c}[\geq 2] = (17.6 \pm 2.8^{+1.5}_{-2.1})$ fb, where $B^{\eta_c}[\geq 2]$ denotes the branching fraction for the η_c decaying into at least two charged tracks. Meanwhile, the NRQCD LO theoretical predictions in the QCD coupling constant α_s and the charm-quark relative velocity v, given by Braaten and Lee [6], Liu, He, and Chao [7], and Hagiwara, Kou, and Qiao [8], are about $2.3 \sim 5.5$ fb, which is an order of magnitude smaller than the experimental results. Such a large discrepancy between experimental results and theoretical predictions brings a challenge to the current understanding of charmonium production based on NRQCD. Many studies have been performed in order to resolve the problem. Braaten and Lee [6] have shown that the relativistic corrections would increase the cross section by a factor of about 2, which boosts the cross section to 7.4 fb. And the next-to-leading-order (NLO) QCD correction of the process has been studied by Zhang, Gao, and Chao [9], which can enhance the cross section with a K factor (the ratio of NLO to LO) of about 2 and reduce the large discrepancy. Again the relativistic corrections have been studied by Bodwin, Kang, Kim, Lee, and Yu [10] and by He, Fan, and Chao [11], which are significant, and when combined with the NLO QCD corrections, may resolve the large discrepancy. In Ref. [12], $\Upsilon(4s) \to J/\psi + \eta_c$ was considered by Jia, but its contribution is small. Ma and Si [13] treated the process by using the light-cone method. A similar treatment was performed by Bondar and Chernyad [14] and Bodwin, Kang, and Lee [15]. More detailed treatment, such as including the resummation of a class of relativistic correction, has been take into consideration by Bodwin, Lee, and Yu [16].

Since the calculation of the NLO QCD correction for this process is quite complicated and plays a very important role in explaining the experimental data, in this paper we perform an independent calculation by using the package Feynman Diagram Calculation (FDC) [17] with a one-loop part built in and obtained analytic result. The numerical result is in agreement with the previous result in Ref. [9].

This paper is organized as follows. In Sec. II, we give the LO cross section for the process. The calculation of NLO QCD corrections is described in Sec. III. In Sec. IV, numerical results are presented. The conclusion and discussion are given in Sec. V. In the appendixes, some useful details are presented.

II. THE LO CROSS SECTION

There are four Feynman diagrams for this order: two are shown in Fig. 1, while the other two can be obtained by reversing the arrows of the quark lines. Momenta for the involved particles are labeled as

$$e^-(p_1) + e^+(p_2) \to J/\psi(p_3) + \eta_c(p_4). \qquad (1)$$

In the nonrelativistic limit, we can use the NRQCD factorization formalism and obtain the square of the scattering amplitude as

$$|M_{\rm LO}|^2 = \frac{2^{14}\pi^2\alpha^2\alpha_s^2 e_c^2 |R_s^{J/\psi}(0)|^2 |R_s^{\eta_c}(0)|^2}{9 m_c^6 s^5} \times (2 - 4s + s^2 - 4t + 2st + 2t^2), \qquad (2)$$

with

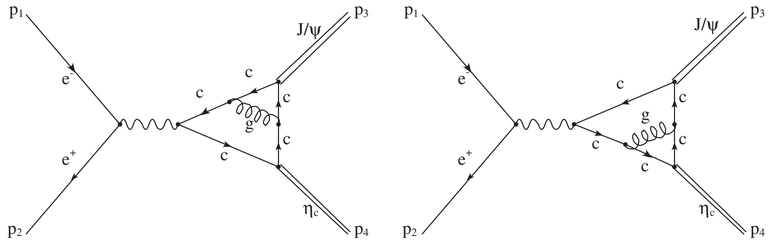

FIG. 1. Feynman diagrams for LO.

$$s = \frac{(p_1 + p_2)^2}{4m_c^2}, \qquad t = \frac{(p_1 - p_3)^2}{4m_c^2}, \tag{3}$$

where $e_c = \frac{2}{3}$ is the electric charge of the charm quark. $R_s^{J/\psi}(0)$ and $R_s^{\eta_c}(0)$ are the radial wave functions at the origin of J/ψ and η_c. Notice that s in Eq. (3) is used from now on. After the integration of phase space, the total cross section is

$$\sigma^{(0)} = \frac{128\pi\alpha^2\alpha_s^2 e_c^2 |R_s^{J/\psi}(0)|^2 |R_s^{\eta_c}(0)|^2 (s-4)^{3/2}}{27 m_c^8 s^{11/2}}. \tag{4}$$

III. THE NLO CROSS SECTION

Since there is no $\mathcal{O}(\alpha_s)$ real process in NLO, we only need to calculate virtual corrections. Dimensional regularization has been adopted for isolating the ultraviolet (UV) and infrared (IR) singularities. UV divergences from self-energy and triangle diagrams are canceled upon the renormalization of the QCD gauge coupling constant, the charm-quark mass and field, and the gluon field. A similar renormalization scheme is chosen as in Ref. [18], except that both light quarks and charm quarks are included in the quark loop to obtain the renormalization constants. The renormalization constants of the charm-quark mass Z_m and field Z_2, and the gluon field Z_3 are defined in the on-mass-shell (OS) scheme, while that of the QCD gauge coupling Z_g is defined in the modified-minimal-subtraction ($\overline{\rm MS}$) scheme:

$$\begin{aligned}
\delta Z_m^{\rm OS} &= -3C_F \frac{\alpha_s}{4\pi}\left[\frac{1}{\epsilon_{\rm UV}} - \gamma_E + \ln\frac{4\pi\mu^2}{m_c^2} + \frac{4}{3} + \mathcal{O}(\epsilon)\right],\\
\delta Z_2^{\rm OS} &= -C_F \frac{\alpha_s}{4\pi}\left[\frac{1}{\epsilon_{\rm UV}} + \frac{2}{\epsilon_{\rm IR}} - 3\gamma_E + 3\ln\frac{4\pi\mu^2}{m_c^2}\right.\\
&\quad \left. + 4 + \mathcal{O}(\epsilon)\right],\\
\delta Z_3^{\rm OS} &= \frac{\alpha_s}{4\pi}\left[(\beta_0' - 2C_A)\left(\frac{1}{\epsilon_{\rm UV}} - \frac{1}{\epsilon_{\rm IR}}\right)\right.\\
&\quad \left. - \frac{4}{3}T_F\left(\frac{1}{\epsilon_{\rm UV}} - \gamma_E + \ln\frac{4\pi\mu^2}{m_c^2}\right) + \mathcal{O}(\epsilon)\right],\\
\delta Z_g^{\overline{\rm MS}} &= -\frac{\beta_0}{2}\frac{\alpha_s}{4\pi}\left[\frac{1}{\epsilon_{\rm UV}} - \gamma_E + \ln(4\pi) + \mathcal{O}(\epsilon)\right],
\end{aligned} \tag{5}$$

where γ_E is Euler's constant, $\beta_0 = \frac{11}{3}C_A - \frac{4}{3}T_F n_f$ is the one-loop coefficient of the QCD beta function, and n_f is the number of active quark flavors. There are three massless light quarks, u, d, s, and one heavy quark, c, so $n_f = 4$. In $SU(3)_c$, color factors are given by $T_F = \frac{1}{2}$, $C_F = \frac{4}{3}$, $C_A = 3$. And $\beta_0' \equiv \beta_0 + (4/3)T_F = (11/3)C_A - (4/3)T_F n_{lf}$, where $n_{lf} \equiv n_f - 1 = 3$ is the number of light quarks flavors. Actually, in the NLO total amplitude level, the terms proportion to $\delta Z_3^{\rm OS}$ cancel each other; thus the result is independent of the renormalization scheme of the gluon field.

After having fixed our renormalization scheme and omitting diagrams that do not contribute, including counterterm diagrams, there are 80 NLO diagrams remaining, which are shown in Fig. 2. They are divided into 13 groups. Diagrams of group (f) and (j) that have a virtual gluon line connected with the quark pair in a meson lead to Coulomb singularity $\sim\pi^2/v$, which can be isolated by introducing a small relative velocity $v = |\vec{p}_c - \vec{p}_{\bar{c}}|$. The corresponding contribution is also of $\mathcal{O}(\alpha_s)$ and can be taken into the $c\bar{c}$ wave function renormalization [19] as

$$\begin{aligned}
\sigma &= |R_s(0)|^2\hat{\sigma}^{(0)}\left(1 + \frac{\alpha_s}{\pi}C_F\frac{\pi^2}{v} + \frac{\alpha_s}{\pi}C + \mathcal{O}(\alpha_s^2)\right)\\
&\Rightarrow |R_s^{\rm ren}(0)|^2\hat{\sigma}^{(0)}\left[1 + \frac{\alpha_s}{\pi}C + \mathcal{O}(\alpha_s^2)\right].
\end{aligned} \tag{6}$$

A factor of 2 should be used since there are two bound states. After adding contributions from all the diagrams together, all the IR-divergent terms are canceled and the total scattering amplitude is obtained as

$$\begin{aligned}
M_{\rm NLO} + M_{\rm LO} = M_{\rm LO}\left\{1 + \frac{\alpha_s(\mu)}{2\pi}\left[\frac{8}{3}\frac{\pi^2}{v} - \beta_0\ln\frac{2m_c}{\mu}\right.\right.\\
\left.\left. + \frac{K_1(s)}{6} + i\pi\frac{K_2(s)}{6}\right]\right\},
\end{aligned} \tag{7}$$

with $K_1(s)$ and $K_2(s)$ given by Eqs. (A1) and (A2).

Meanwhile, α_s should be obtained from a two-loop formula as

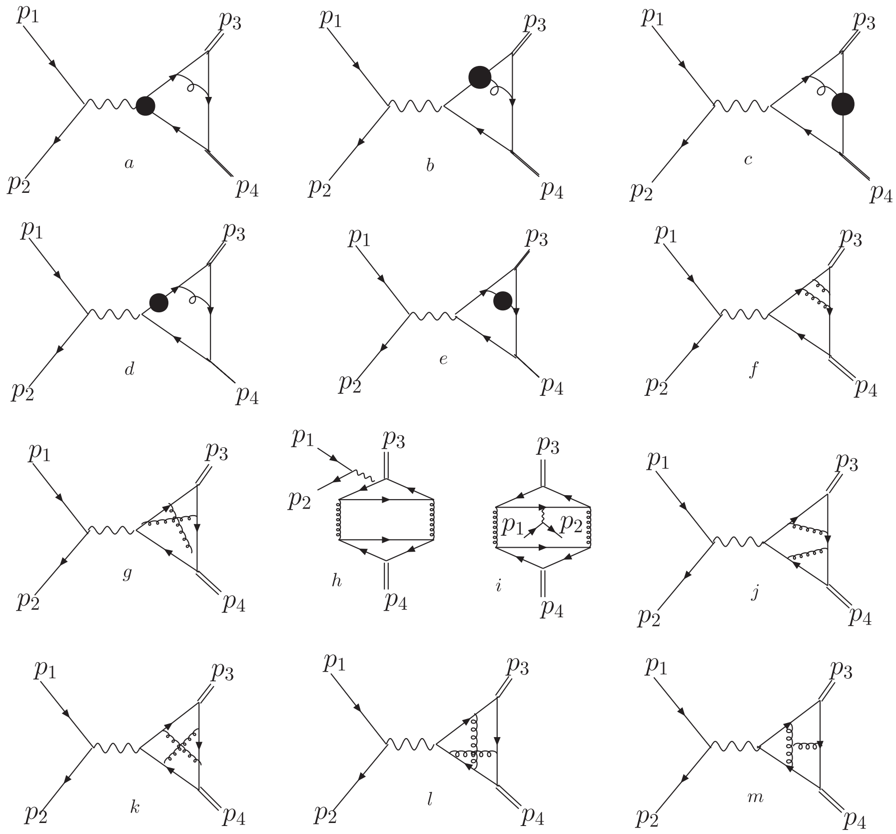

FIG. 2. All Feynman diagrams for NLO are divided into 13 groups. (a) includes the photon-quark vertex counterterm and the corresponding loop diagrams; (b) and (c) are the gluon-quark vertex counterterm and the corresponding loop diagrams; (d) and (e) denote the counterterm and the corresponding loop diagrams for the quark and gluon self-energy; (f) and (j) are diagrams that contain Coulomb singularity. Other diagrams can be obtained by reversing the arrows of quark lines and/or changing the locations of J/ψ and η_c. But notice that we cannot change the locations of J/ψ and η_c in groups (h) and (i).

$$\frac{\alpha_s(\mu)}{4\pi} = \frac{1}{\beta_0 \ln(\mu^2/\Lambda_{\rm QCD}^2)} - \frac{\beta_1 \ln\ln(\mu^2/\Lambda_{\rm QCD}^2)}{\beta_0^3 \ln^2(\mu^2/\Lambda_{\rm QCD}^2)}, \quad (8)$$

where $\beta_1 = 34C_A^2/3 - 4(C_F + 5C_A/3)T_F n_f$ is the two-loop coefficient of the QCD beta function. From Eq. (7) the total cross section at NLO is

$$\sigma_{\rm NLO} = \sigma^{(0)}\left\{1 + \frac{\alpha_s(\mu)}{\pi}\left[-\beta_0 \ln\frac{2m_c}{\mu} + \frac{K_1(s)}{6}\right]\right\}. \quad (9)$$

IV. NUMERICAL RESULT

Up to NLO, the value of the wave function at the origin of J/ψ is related to the leptonic decay widths as

$$\Gamma_{ee} = \left(1 - \frac{16}{3}\frac{\alpha_s}{\pi}\right)\frac{4\alpha^2 e_c^2}{M_{J/\psi}^2}|R_s^{J/\psi}(0)|^2, \quad (10)$$

and according to Ref. [1], we can set $R_s^{\eta_c}(0) = R_s^{J/\psi}(0) = R_s(0)$. If we choose $|R_s(0)|^2 = 0.978\ \text{GeV}^3$ and $\Lambda_{\overline{\rm MS}}^{(4)} = 0.338$ GeV, then we get the numerical result shown in Table I, which is consistent with the result in Ref. [9].

V. CONCLUSION

We calculated the NLO QCD correction of J/ψ plus η_c production in e^+e^- annihilation at center-of-mass energy 10.6 GeV. The method of dimensional regulariza-

TABLE I. Cross sections with different charm-quark mass m_c and renormalization scale μ. $\sqrt{s_0} = 10.6$ GeV is the center-of-mass energy.

m_c (GeV)	μ	$\alpha_s(\mu)$	$\sigma_{\rm LO}$ (fb)	$\sigma_{\rm NLO}$ (fb)	$\sigma_{\rm NLO}/\sigma_{\rm LO}$
1.5	m_c	0.369	16.09	27.51	1.710
1.5	$2m_c$	0.259	7.94	15.68	1.975
1.5	$\sqrt{s_0}/2$	0.211	5.27	11.14	2.114
1.4	m_c	0.386	19.28	34.92	1.811
1.4	$2m_c$	0.267	9.19	18.84	2.050
1.4	$\sqrt{s_0}/2$	0.211	5.76	12.61	2.189

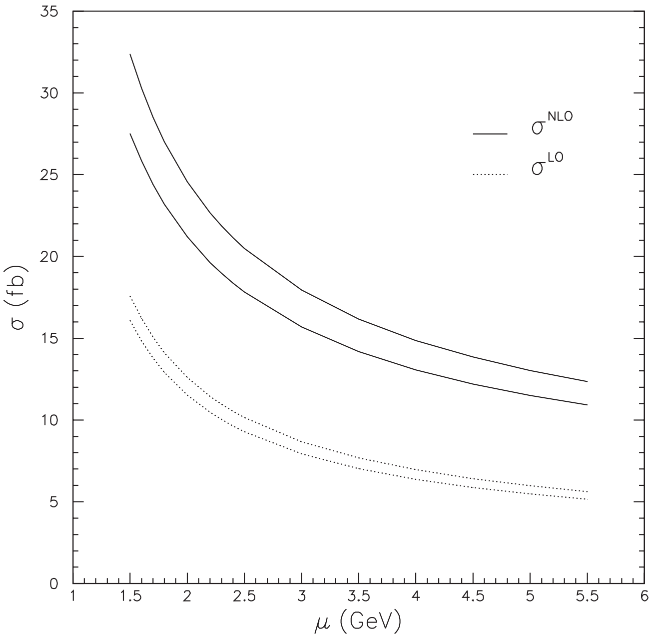

FIG. 3. Cross sections as a function of the renormalization scale μ with $|R_s(0)|^2 = 0.978\ \mathrm{GeV}^3$, $\Lambda = 0.338\ \mathrm{GeV}$, and center-of-mass energy 10.6 GeV. The charm-quark mass is chosen as 1.4 GeV (upper curves) and 1.5 GeV (lower curves).

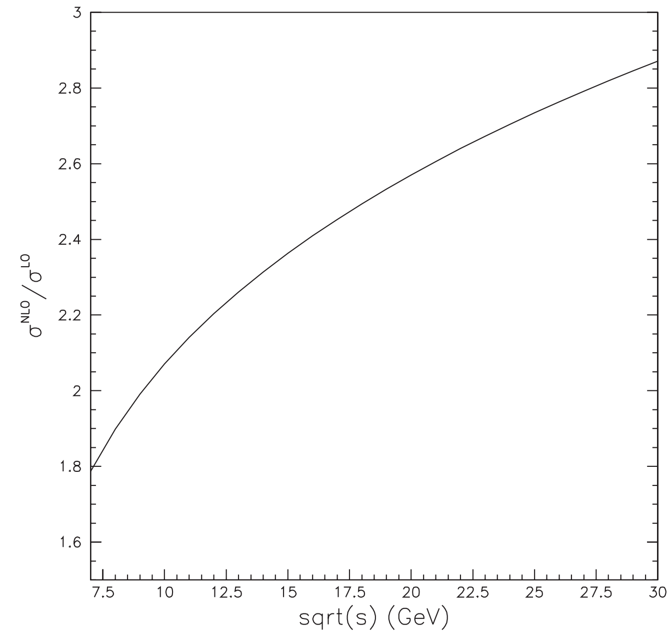

FIG. 5. The K factor as a function of the center-of-mass energy with $|R_s(0)|^2 = 0.978\ \mathrm{GeV}^3$ and $\Lambda = 0.338\ \mathrm{GeV}$. The renormalization scale μ is set at half of the center-of-mass energy and $m_c = 1.5\ \mathrm{GeV}$.

tion is taken to deal with the UV and IR singularities, and the Coulomb singularity is isolated by a small

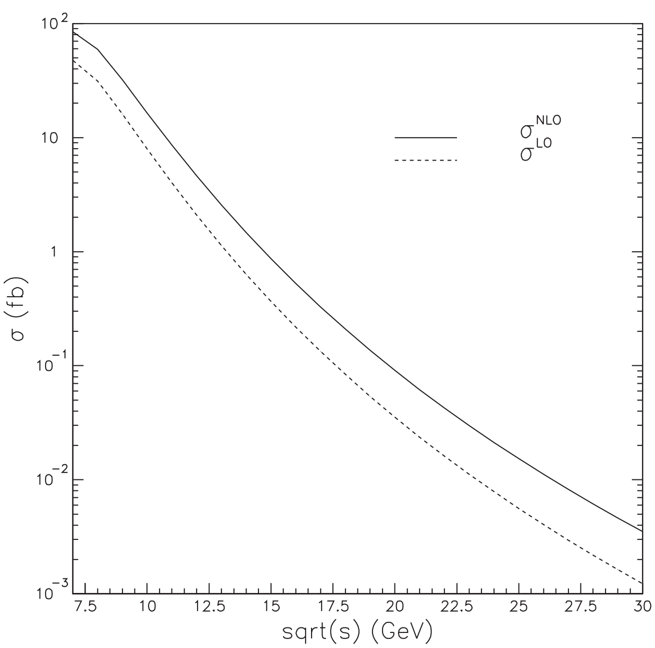

FIG. 4. Cross sections as a function of the center-of-mass energy with $|R_s(0)|^2 = 0.978\ \mathrm{GeV}^3$ and $\Lambda = 0.338\ \mathrm{GeV}$. The renormalization scale μ is set at half of the center-of-mass energy and $m_c = 1.5\ \mathrm{GeV}$.

relative velocity v between the charm-quark pair in the meson and absorbed into the $c\bar{c}$ bound state wave function. After taking all one-loop diagrams into account, an analytic finite result is obtained. By choosing proper physical parameters, we get a K factor (ratio of NLO to LO) of about 2, which is consistent with Ref. [9]. It decreases the great discrepancy between theory and experiment. From Fig. 3, it could be found that the dependence on the renormalization scale μ has not been improved in the NLO calculation. The plot of the total cross section vs the center-of-mass energy of e^+e^- in Fig. 4 behaves as expected. But the plot of the K factor vs the center-of-mass energy of e^+e^- in Fig. 5 shows that it is more difficult to obtain the convergent result from the perturbative QCD without resummation of $\ln\frac{s}{m_c^2}$ terms as the center-of-mass energy of e^+e^- becomes larger.

ACKNOWLEDGMENTS

This work was supported by the National Natural Science Foundation of China (No. 10475083).

APPENDIX A: THE DEFINITION OF K_1 AND K_2

In this section, the definitions $K_1(s)$ and $K_2(s)$ used in Eq. (7) are presented.

$$
\begin{aligned}
K_1(s) = {} & \frac{-24-79s-68s^2}{3s(2s+1)} + f_1\frac{s^2-3s+16}{2(s-4)} - f_2\frac{3s}{2(s-2)} + f_3\frac{-34s^3+193s^2-342s+160}{4(s-4)(s-2)} \\
& + f_4\frac{-41s^2-194s+64}{32(s-4)} + f_5\frac{8s^2-21s-8}{2(s-4)} + f_6\frac{65s^2-302s+64}{32(s-4)} + f_7\frac{-3s^2-4s}{2(s-4)} \\
& + a_1\left[\frac{4z_1(8-7s)}{s^2(s-4)} + \frac{-64s^4+406s^3+11s^2-335s-120}{(s-4)(2s+1)^2}\right] + a_6\left[\frac{2z_1(8-7s)}{s^2(s-4)} + \frac{z_2(-130+19s+8s^2)}{s(s-4)}\right. \\
& \left. + \frac{-32s^4-110s^3+639s^2+696s+172}{(s-4)(2s+1)^2}\right] + a_7\frac{4z_1(7s-8)}{s^2(s-4)} + a_9\frac{2z_2(-8s^2-19s+130)}{s(s-4)},
\end{aligned}
\tag{A1}
$$

$$
\begin{aligned}
K_2(s) = {} & 2z_1\frac{-7s+8}{(s-4)s^2} + z_2\frac{-8s^2-19s+130}{(s-4)s} + \frac{32s^4+110s^3-639s^2-696s-172}{(s-4)(2s+1)^2} + z_1\frac{(65s^2-302s+64)}{4s(s-4)^2}a_{13} \\
& + z_1\frac{(21s^3-64s^2-1396s+2688)}{8(s-2)s(s-4)^2}a_1 + z_1\frac{(73s^3-96s^2+444s-896)}{8(s-2)s(s-4)^2}a_3 \\
& - z_1\frac{(193s^3-1292s^2+2548s-1280)}{8(s-2)s(s-4)^2}a_5 + z_1\frac{(79s^2-82s+64)}{8s(s-4)^2}a_6 - 4z_1\frac{(8s^2-21s-8)}{s(s-4)^2}a_7 \\
& + z_1\frac{(34s^3-193s^2+342s-160)}{2(s-2)s(s-4)^2}(a_{10}-a_8) + z_1\frac{(183s^3-1624s^2+3316s-1408)}{8(s-2)s(s-4)^2}a_{12},
\end{aligned}
\tag{A2}
$$

where all the variables used in $K_1(s)$ and $K_2(s)$ are defined as

$$
z_1 = \sqrt{s^2-4s}, \qquad z_2 = \sqrt{s^2-s},
\tag{A3}
$$

$$
\begin{aligned}
f_1 &= \frac{4z_1}{s^2-4s}(-2a_1^2 - a_1a_2 - a_1a_3 + a_1a_4 + 2a_1a_6 + 4a_1a_7 - a_2a_3 + a_3^2 + a_3a_4 - a_3a_5 - 2a_3a_6 + a_5a_6 \\
&\quad + a_6^2 - 2a_6a_7 - l_1 + l_2 - l_3 - l_4 + l_5 - l_6 + l_7 + 2l_8), \\
f_2 &= \frac{2z_1}{s^2-4s}(6a_1^2 - 2a_1a_3 + a_1a_5 - 4a_1a_7 - 2a_3a_6 + a_5a_6 - 2a_6^2 + 4a_6a_7 + l_{10} - l_{11} - l_{12} + l_{13} + 2l_{14} - l_9), \\
f_3 &= \frac{2z_1}{s^2-4s}(2a_1a_{12} - a_1a_5 + a_{10}a_6 - 2a_{10}a_9 - 2a_{11}a_{12} - 2a_{12}^2 + 2a_{12}a_5 + 2a_{12}a_6 + 2a_{12}a_7 - a_5a_6 - a_6a_8 \\
&\quad + 2a_8a_9 - 2l_{15} + l_{16} + l_{17} + l_{18} - l_{19} - l_{20} + l_{21} - l_{22}), \\
f_4 &= \frac{4z_1}{s^2-4s}(-2a_1a_{12} + a_1a_5 - a_1a_6 - a_{12}a_6 + a_3a_6 - 2l_{15} + l_{23} + l_{24} - l_{25} - l_{26} + l_{27}), \\
f_5 &= \frac{4z_1}{s^2-4s}(-2a_1a_6 - a_6^2 + 2a_6a_7 - 2l_{15} + l_{26} - l_{27} + 2l_{28}), \\
f_6 &= \frac{4z_1}{s^2-4s}(-2a_1a_{13} + a_1a_5 + 2a_1a_6 + 2a_1a_7 - 2a_{13}a_6 + a_5a_6 + a_6^2 - l_{16} - l_{21} + l_{22} - l_{26} + l_{27} + 2l_{28}), \\
f_7 &= \frac{2z_1}{s^2-4s}(-2a_1a_{14} + 2a_1a_{15} - a_1a_5 + a_{12}^2 - a_{12}a_{14} + a_{12}a_{15} - a_{12}a_5 - 2a_{12}a_6 + a_5a_6 - 2l_{15} - l_{16} - l_{21} \\
&\quad + l_{22} + 4l_{28}),
\end{aligned}
\tag{A4}
$$

$$
\begin{aligned}
& a_1 = \mathrm{a}\ln(2), \quad a_2 = \mathrm{a}\ln(s^2 - sz_1 - 2z_1), \quad a_3 = \mathrm{a}\ln(s - z_1 + 2), \quad a_4 = \mathrm{a}\ln(s^2 - sz_1 + 2s - z_1), \\
& a_5 = \mathrm{a}\ln(2s+1), \quad a_6 = \mathrm{a}\ln(s), \quad a_7 = \mathrm{a}\ln(s+z_1), \quad a_8 = \mathrm{a}\ln(3s^2 + sz_1 - sz_2 - 6s - 3z_1z_2 - 2z_1 + 4z_2), \\
& a_9 = \mathrm{a}\ln(s - z_2), \quad a_{10} = \mathrm{a}\ln(3s^2 + sz_1 + sz_2 - 6s + 3z_1z_2 - 2z_1 - 4z_2), \quad a_{11} = \mathrm{a}\ln(2s^2 + 2sz_1 - 5s - z_1), \\
& a_{12} = \mathrm{a}\ln(s - z_1 - 1), \quad a_{13} = \mathrm{a}\ln(3s - z_1), \quad a_{14} = \mathrm{a}\ln(s^2 - sz_1 - 3s + z_1), \quad a_{15} = \mathrm{a}\ln(s^2 - sz_1 - s - z_1),
\end{aligned}
\tag{A5}
$$

and

$$l_1 = \mathrm{Li}_2^r\left(\frac{s^2 + sz_1 - 4s + 2z_1}{8s^2 + 4s}\right), \quad l_2 = \mathrm{Li}_2^r\left(\frac{-s^2 - sz_1 + 4s - 2z_1}{4s + 2}\right), \quad l_3 = \mathrm{Li}_2^r\left(\frac{-s^2 + sz_1 + 4s + 2z_1}{4s}\right),$$
$$l_4 = \mathrm{Li}_2^r\left(\frac{-s - z_1 + 4}{8}\right), \quad l_5 = \mathrm{Li}_2^r\left(\frac{-s + z_1 + 4}{8}\right), \quad l_6 = \mathrm{Li}_2^r\left(\frac{s - z_1 - 4}{2s}\right),$$
$$l_7 = \mathrm{Li}_2^r\left(\frac{s + z_1 - 4}{2s}\right), \quad l_8 = \mathrm{Li}_2^r\left(\frac{z_1}{2s}\right), \quad l_9 = \mathrm{Li}_2^r\left(\frac{s^3 + s^2z_1 - 4s^2 - 2sz_1 - 2z_1}{8s + 4}\right),$$
$$l_{10} = \mathrm{Li}_2^r\left(\frac{-s^4 - s^3z_1 + 4s^3 + 2s^2z_1 + 2sz_1}{4s + 2}\right), \quad l_{11} = \mathrm{Li}_2^r\left(\frac{-s^3 + s^2z_1 + 4s^2 - 2sz_1 - 2z_1}{4}\right),$$
$$l_{12} = \mathrm{Li}_2^r\left(\frac{-s^2 - sz_1 + 4s + 2z_1}{2}\right), \quad l_{13} = \mathrm{Li}_2^r\left(\frac{-s^2 + sz_1 + 4s - 2z_1}{2}\right), \quad l_{14} = \mathrm{Li}_2^r\left(\frac{z_1}{2}\right),$$
$$l_{15} = \mathrm{Li}_2^r\left(\frac{-z_1}{s}\right), \quad l_{16} = \mathrm{Li}_2^r\left(\frac{s^2 + sz_1 - 4s - z_1}{2s^2 + s}\right), \quad l_{21} = \mathrm{Li}_2^r\left(\frac{-s^2 + sz_1 + 4s - z_1}{s}\right),$$
$$l_{22} = \mathrm{Li}_2^r\left(\frac{-2s^2 - 2sz_1 + 8s + 2z_1}{2s + 1}\right), \quad l_{23} = \mathrm{Li}_2^r\left(\frac{s^2 - sz_1 - 4s + z_1}{2s^2 + s}\right), \quad l_{24} = \mathrm{Li}_2^r\left(\frac{-s^2 - sz_1 + 4s + z_1}{s}\right), \tag{A6}$$
$$l_{25} = \mathrm{Li}_2^r\left(\frac{-2s^2 + 2sz_1 + 8s - 2z_1}{2s + 1}\right), \quad l_{26} = \mathrm{Li}_2^r\left(\frac{-s - z_1 + 4}{2}\right), \quad l_{27} = \mathrm{Li}_2^r\left(\frac{-s + z_1 + 4}{2}\right),$$
$$l_{28} = \mathrm{Li}_2^r\left(\frac{z_1}{s}\right), \quad l_{17} = \mathrm{Li}_2^r\left(\frac{-s^3 - s^2z_1 - s^2z_2 + 5s^2 - sz_1z_2 + 2sz_1 + 4sz_2 - 4s + 2z_1z_2}{s^2}\right),$$
$$l_{18} = \mathrm{Li}_2^r\left(\frac{-s^3 - s^2z_1 + s^2z_2 + 5s^2 + sz_1z_2 + 2sz_1 - 4sz_2 - 4s - 2z_1z_2}{s^2}\right),$$
$$l_{19} = \mathrm{Li}_2^r\left(\frac{-s^3 + s^2z_1 - s^2z_2 + 5s^2 + sz_1z_2 - 2sz_1 + 4sz_2 - 4s - 2z_1z_2}{s^2}\right),$$
$$l_{20} = \mathrm{Li}_2^r\left(\frac{-s^3 + s^2z_1 + s^2z_2 + 5s^2 - sz_1z_2 - 2sz_1 - 4sz_2 - 4s + 2z_1z_2}{s^2}\right).$$

In the above expressions, $a\ln(x) = \ln|x|$ and $\mathrm{Li}_2^r(x) = \mathrm{Re}[\mathrm{Li}_2(x)]$.

APPENDIX B: THE RESULTS FOR ALL THE SCALAR INTEGRALS

In this section, we present the results of scalar integrals. Functions A to E denote one- to five-point scalar integrals, and variables of the functions are written as $T(p_0, m_0, \ldots, p_n, m_n)$ where p_i and m_i denote parameters of the nth propagator $N_i = (q + p_i)^2 - m_i^2 + i\epsilon$. q is the loop momentum, and a factor of

$$C_\epsilon = \frac{i}{16\pi^2} e^{-\epsilon\gamma_E}\left(\frac{4\pi\mu^2}{4m_c^2}\right) \tag{B1}$$

is taken away from all the scalar integrals.

We have developed a full series of methods in calculating tensor and scalar integrals with dimensional regularization and realized it in FDC [17]. A paper about these methods is in preparation. All the scalar integrals are calculated analytically by using FDC, and the results are shown in the following.

One-point scalar integrals:

$$A(0, m_c) = 4F_{14}m_c^2 + \frac{1}{\varepsilon_{\rm UV}} m_c^2. \tag{B2}$$

Two-point scalar integrals:

$$\begin{aligned} B\left(0, 0, \frac{2p_3 + p_4}{2}, m_c\right) &= F_{13} + \frac{1}{\varepsilon_{\rm UV}}, \\ B\left(0, 0, \frac{-p_3 - p_4}{2}, 0\right) &= F_{12} + \frac{1}{\varepsilon_{\rm UV}}, \\ B\left(0, m_c, \frac{p_3 + p_4}{2}, m_c\right) &= F_{11} + \frac{1}{\varepsilon_{\rm UV}}, \\ B(0, m_c, p_3 + p_4, m_c) &= F_{10} + \frac{1}{\varepsilon_{\rm UV}}, \\ B\left(0, 0, \frac{p_4}{2}, m_c\right) &= F_9 + \frac{1}{\varepsilon_{\rm UV}}. \end{aligned} \tag{B3}$$

Three-point scalar integrals:

$$
\begin{aligned}
&C\left(0,0,\frac{p_3}{2},m_c,\frac{-p_3}{2},m_c\right)=\frac{1}{4m_c^2}\left(F_8-\frac{2\pi^2}{v}-\frac{2}{\varepsilon_{\rm IR}}\right), \qquad C\left(0,0,\frac{p_4}{2},m_c,\frac{2p_3+p_4}{2},m_c\right)=\frac{1}{4m_c^2}F_7,\\
&C\left(0,0,\frac{-p_4}{2},m_c,\frac{p_3+p_4}{2},0\right)=\frac{1}{4m_c^2}F_6, \qquad C\left(0,0,\frac{p_3}{2},m_c,\frac{p_3+p_4}{2},0\right)=\frac{1}{4m_c^2}F_5,\\
&C\left(0,0,\frac{2p_3+p_4}{2},m_c,\frac{p_3+p_4}{2},0\right)=\frac{1}{4m_c^2}F_4, \qquad C\left(0,0,\frac{p_3+2p_4}{2},m_c,\frac{-p_3}{2},m_c\right)=\frac{1}{4m_c^2}F_3,\\
&C\left(0,0,\frac{p_3}{2},m_c,-p_4,0\right)=\frac{1}{4m_c^2}F_2, \qquad C\left(0,0,\frac{p_4}{2},m_c,\frac{p_3+2p_4}{2},m_c\right)=\frac{1}{4m_c^2}F_1.
\end{aligned} \tag{B4}
$$

Four-point scalar integrals:

$$
\begin{aligned}
&D\left(0,0,\frac{2p_3+p_4}{2},m_c,\frac{-p_4}{2},m_c,\frac{p_4}{2},m_c\right)=\frac{1}{16m_c^4s}\left(F_{15}s-\frac{4\pi^2}{v}-\frac{4}{\varepsilon_{\rm IR}}\right),\\
&D\left(0,0,\frac{p_3}{2},m_c,\frac{-p_3}{2},m_c,\frac{-p_3-p_4}{2},0\right)=\frac{1}{16m_c^4s}\left(F_{16}s-\frac{8\pi^2}{v}-\frac{8}{\varepsilon_{\rm IR}}\right),\\
&D\left(0,0,\frac{-p_4}{2},m_c,\frac{2p_3+p_4}{2},m_c,\frac{p_3+p_4}{2},0\right)=\frac{1}{16m_c^4}F_{17}.
\end{aligned} \tag{B5}
$$

Five-point scalar integrals:

$$
E\left(0,0,\frac{-p_3}{2},m_c,\frac{-p_3-2p_4}{2},m_c,\frac{p_3}{2},m_c,\frac{-p_3-p_4}{2},0\right)=\frac{1}{64m_c^6s^2}\left(F_{18}s^2-\frac{32\pi^2}{v}-\frac{32}{\varepsilon_{\rm IR}}\right). \tag{B6}
$$

And here are the results for F_i, where f_i and a_i are defined as before.

$$
\begin{aligned}
&F_1=\frac{1}{s(s-4)}4\pi i z_1(a_6-a_5+2a_3-4a_1)+f_1, \qquad F_2=\frac{1}{s(s-4)}2\pi i z_1(-a_5+2a_3-2a_1)+f_2,\\
&F_3=\frac{1}{s(s-4)}2\pi i z_1(-2a_{12}-a_{10}+a_8+a_5)+f_3, \qquad F_4=\frac{1}{s(s-4)}4\pi i z_1(a_{12}-a_3+a_1)+f_4,\\
&F_5=\frac{1}{s(s-4)}4\pi i z_1(-2a_7+a_6+2a_1)+f_5, \qquad F_6=\frac{1}{s(s-4)}4\pi i z_1(2a_{13}-a_6-a_5-2a_1)+f_6,\\
&F_7=\frac{1}{s(s-4)}2\pi i z_1(2a_{12}-a_5)+f_7, \qquad F_8=2(-2a_1+2),\\
&F_9=2(a_1+1), \qquad F_{10}=\frac{1}{s}[z_2(2a_9-a_6+i\pi)+2(a_1s+s)],\\
&F_{11}=\frac{1}{s}[z_1(-2a_7+a_6+2a_1+i\pi)+2(a_1s+s)], \qquad F_{12}=-a_6+2a_1+i\pi+2,\\
&F_{13}=\frac{1}{2s+1}[2a_1(s+1)+2(-a_6s+i\pi s+2s+1)], \qquad F_{14}=\frac{1}{4}(2a_1+1),\\
&F_{15}=\frac{1}{s^2}[8\pi i(-s+z_2)+8z_2(2a_9-a_6)+8s(a_6+1)], \qquad F_{16}=\frac{1}{s}(-32a_1+16),\\
&F_{17}=\frac{1}{s^2}[16\pi i(-s+z_2)+16z_2(2a_9-a_6)+16(a_6s+2a_1s)],\\
&F_{18}=\frac{1}{s^3}[32\pi i(s-2)(s-z_2)+32z_2(s-2)(-2a_9+a_6)-32a_6s(s-2)-64a_1s^2+64s].
\end{aligned} \tag{B7}
$$

APPENDIX C: THE SCHEME TO TREAT γ_5 IN D DIMENSION

As we all know, there is no explicit definition for γ_5 in D dimensions. Usually the following relations are used when one encounters γ_5 in D dimensions:

$$\{\gamma_5, \gamma_\mu\} = 0, \tag{C1}$$

$$\mathrm{Tr}\,(\gamma_5 \hat{p}_1 \hat{p}_2 \hat{p}_3 \hat{p}_4) = 4i\epsilon_{\mu\nu\alpha\beta} p_1^\mu p_2^\nu p_3^\alpha p_4^\beta. \tag{C2}$$

Notice that $\epsilon_{\mu\nu\alpha\beta}$ goes to zero when any of its indices is out of the 4 dimensions.

While calculating the trace of the product of several matrices that contain γ_5 and indices in D dimensions, different ways may lead to different results. For example, when calculating the trace of matrix $M = \gamma_5\gamma_\mu \hat{p}_1 \hat{p}_2 \hat{p}_3 \hat{p}_4 \gamma^\mu$, we have two different routes as shown in Fig. 6:

(1) In route A_1, the summing up of the index μ does not go across γ_5.

$$\begin{aligned} \mathrm{Tr}\,(M)|_{A_1} &= \mathrm{Tr}\{\gamma_5[(D-2)\hat{p}_1 \hat{p}_2 \hat{p}_3 \hat{p}_4 \\ &\quad + 2\hat{p}_2 \hat{p}_1 \hat{p}_3 \hat{p}_4 - 2\hat{p}_3 \hat{p}_1 \hat{p}_2 \hat{p}_4 \\ &\quad + 2\hat{p}_4 \hat{p}_1 \hat{p}_2 \hat{p}_3]\} \\ &= 4i(D-8)\epsilon_{\mu\nu\alpha\beta} p_1^\mu p_2^\nu p_3^\alpha p_4^\beta. \end{aligned} \tag{C3}$$

(2) In route A_2, it does go across γ_5.

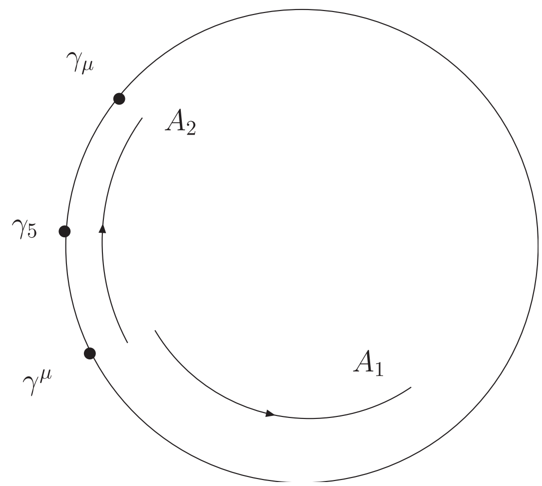

FIG. 6. Trace calculation including γ_5.

$$\begin{aligned} \mathrm{Tr}\,(M)|_{A_2} &= -\mathrm{Tr}(\gamma_5\gamma^\mu\gamma_\mu \hat{p}_1 \hat{p}_2 \hat{p}_3 \hat{p}_4) \\ &= -D\,\mathrm{Tr}(\gamma_5 \hat{p}_1 \hat{p}_2 \hat{p}_3 \hat{p}_4) \\ &= -4iD\epsilon_{\mu\nu\alpha\beta} p_1^\mu p_2^\nu p_3^\alpha p_4^\beta. \end{aligned} \tag{C4}$$

It is easy to find that $\mathrm{Tr}(M)|_{A_1} = \mathrm{Tr}(M)|_{A_2}$ in 4 dimensions, but in D dimensions they are different from each other. So we should always take the same route when dealing with traces containing γ_5 in order to keep our final finite result consistent. In FDC, route A_1 is taken.

[1] G. T. Bodwin, E. Braaten, and G. P. Lepage, Phys. Rev. D **51**, 1125 (1995).
[2] A. Abulencia *et al.* (CDF Collaboration), Phys. Rev. Lett. **99**, 132001 (2007).
[3] K. Abe *et al.* (Belle Collaboration), Phys. Rev. Lett. **89**, 142001 (2002).
[4] P. Pakhlov (Belle Collaboration), arXiv:hep-ex/0412041.
[5] B. Aubert *et al.* (*BABAR* Collaboration), Phys. Rev. D **72**, 031101 (2005).
[6] E. Braaten and J. Lee, Phys. Rev. D **67**, 054007 (2003).
[7] K.-Y. Liu, Z.-G. He, and K.-T. Chao, Phys. Lett. B **557**, 45 (2003).
[8] K. Hagiwara, E. Kou, and C.-F. Qiao, Phys. Lett. B **570**, 39 (2003).
[9] Y.-J. Zhang, Y.-j. Gao, and K.-T. Chao, Phys. Rev. Lett. **96**, 092001 (2006).
[10] G. T. Bodwin, D. Kang, T. Kim, J. Lee, and C. Yu, AIP Conf. Proc. **892**, 315 (2007).
[11] Z.-G. He, Y. Fan, and K.-T. Chao, Phys. Rev. D **75**, 074011 (2007).
[12] Y. Jia, Phys. Rev. D **76**, 074007 (2007).
[13] J. P. Ma and Z. G. Si, Phys. Rev. D **70**, 074007 (2004); Phys. Lett. B **647**, 419 (2007).
[14] A. E. Bondar and V. L. Chernyad, Phys. Lett. B **612**, 215 (2005).
[15] G. T. Bodwin, D. Kang, and J. Lee, Phys. Rev. D **74**, 114028 (2006).
[16] G. T. Bodwin, J. Lee, and C. Yu, arXiv:0710.0995.
[17] J.-X. Wang, Nucl. Instrum. Methods Phys. Res., Sect. A **534**, 241 (2004).
[18] M. Klasen, B. A. Kniehl, L. N. Mihaila, and M. Steinhauser, Nucl. Phys. **B713**, 487 (2005).
[19] M. Kramer, Nucl. Phys. **B459**, 3 (1996).